Angle-Selected ^{14}N-ENDOR Study of Copper(II) Complexes with Distorted N_2S_2 and N_2O_2 Coordination Structures

Ryo Miyamoto, Yasunori Ohba, and Masamoto Iwaizumi*

Institute for Chemical Reaction Science, Tohoku University, Katahira, Sendai 980, Japan

Received August 22, 1991

^{14}N hyperfine coupling (HFC) tensors of some copper(II) complexes having tetrahedrally distorted N_2S_2 and N_2O_2 and trigonal bipyramidal N_2O–O_2 coordination structures were examined by the angle-selected ENDOR method. By the use of this spectroscopic method, not only the principal values but also the relative orientations with respect to the **g** tensors were determined from disordered systems. On the basis of the observed ^{14}N HFC tensors, (1) the effects of tetrahedral distortion on ^{14}N HFC constants and the unpaired electron distribution, (2) hybridization of the nitrogen coordinating orbitals, and (3) orientations of the **g** tensor and the copper unpaired electron orbital in the molecular framework were discussed. In the tetrahedrally distorted *cis*-N_2S_2 type complexes, the $g_\perp$ plane was found to be on the S–Cu–S plane. This is attributed to that the orientation of the copper unpaired electron orbital (3d orbital) is tilting toward the S–Cu–S plane and also to that the spin–orbit interactions of the coordinating sulfurs contribute appreciably to the **g** tensor. The obtained information will be useful for studies of electronic states of the copper binding sites in copper proteins, most of which have distorted coordination structures.

Introduction

A lot of investigations have been attempted to obtain detailed structural information from paramagnetic metal complexes in orientationally disordered form, because there are many cases in which interests are taken in complexes in solution or complexes whose crystal samples are not easily available such as most of biological samples. Angle-selected ENDOR is one of the most useful methods for these studies.[1-4] The method gives information not only on the principal values of hyperfine coupling (HFC), nuclear quadrupole coupling (NQC), and the *g* factor but also on their relative orientations.

In this work, we attempted to apply the method to investigate the electronic state of the copper unpaired electron orbitals and their relative orientation with respect to the coordination structures of some copper(II) complexes with distorted coordination structures. The measurements were applied for the complexes having N_2S_2 and N_2O_2 donor sets. The study of the electronic structure of the copper ions in such distorted coordination environments is of particular significance, since the copper binding sites in most copper proteins are considered to have more or less distorted coordination structures and the structures would have some correlation with their enzymatic functions.[5]

Experimental Section

Sample Preparation. All the ligands except for H_2sacen (Figure 1) were synthesized by mixing the appropriate ketones (salicylaldehyde, 2-hydroxyacetophenone, acetylacetone) and amines (alkylamines, alkyldiamines).[8-14] H_2sacen was synthesized by the method in the literature.[6,7] The metal complexes were prepared according to the literature[6-14] and identified by elemental analyses. The copper(II) complexes were doped in planar nickel(II) complexes or tetrahedrally distorted nickel(II) or zinc(II) complexes by recrystallization in concentrations of 1–5%. Doping in complexes with distorted structures allows the formation of distorted copper binding sites.[6-14] Distortion were qualitatively confirmed by the compound EPR parameters ($g_\parallel$ and $^{Cu}A_\parallel$) on the basis of the correlation between the EPR parameters and the coordination structures.[15,16] The parameters for the complexes and their coordination structures are summarized in Table I.

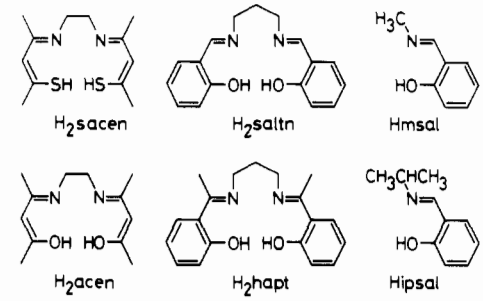

Figure 1. Ligands: H_2sacen, *N*,*N*′-ethylenebis(thioacetylacetone imine); H_2acen, *N*,*N*′-ethylenebis(acetylacetoneimine); H_2saltn, *N*,*N*′-trimethylenebis(salicylaldimine); H_2hapt, bis(2-hydroxyacetophenone) trimethylenediimine; Hmsal, *N*-methylsalicylaldimine; Hipsal, *N*-isopropylsalicylaldimine.

EPR and ENDOR Measurements. EPR spectra were recorded on a Varian E112 X-band EPR spectrometer, and the temperature was controlled at 10–30 K by an Oxford ESR-9 helium-flow cryostat. The magnetic fields and microwave frequencies were measured by an Echo

(1) (a) Hurst, G. C.; Henderson, T. A.; Kreilick, R. W. *J. Am. Chem. Soc.* **1985**, *107*, 7294. (b) Henderson, T. A.; Hurst, G. C.; Kreilick, R. W. *J. Am. Chem. Soc.* **1985**, *107*, 7299.
(2) Yordanov, N. D.; Zdravkova, M.; Shopov, D. *Chem. Phys. Lett.* **1986**, *124*, 191.
(3) (a) Hoffman, B. M.; Martinsen, J.; Venters, R. A. *J. Magn. Reson.* **1984**, *59*, 110. (b) Hoffman, B. M.; Venters, R. A.; Martinsen, J. *J. Magn. Reson.* **1985**, *62*, 537.
(4) Van Willigen, H. *Chem. Phys. Lett.* **1979**, *65*, 490.
(5) (a) Lappin, A. G. In *Metal Ions in Biological Systems*; Sigel, H., Ed.; Marcel Dekker: New York, 1981; Vol. 13, pp 15–71. (b) Solomon, E. I.; Penfield, K. W.; Wilcox, D. E. *Struct. Bonding (Berlin)* **1983**, *53*, 1.
(6) Attanasio, D.; Dessy, G.; Fares, V.; Pennesi, G. *Mol. Phys.* **1980**, *40*, 269.
(7) Cini, R.; Cinquantini, A.; Orioli, P.; Sabat, M. *Inorg. Chim. Acta* **1980**, *41*, 151.
(8) Cariati, F.; Morazzoni, F.; Busetto, C.; Del Piero, C.; Zazzetta, A. *J. Chem. Soc., Dalton Trans.* **1976**, 342.
(9) Fox, M. R.; Lingafelter, E. C. *Acta Crystallogr.* **1967**, *22*, 943.
(10) (a) Iida, K.; Oonishi, I.; Nakahara, A.; Komiyama, Y. *Bull. Chem. Soc. Jpn.* **1970**, *43*, 2347. (b) Scullane, M. I.; Allen, H. C., Jr. *J. Coord. Chem.* **1978**, *8*, 87.
(11) Drew, M. G. B.; Prasad, R. N.; Sharma, R. P. *Acta Crystallogr.* **1985**, *C41*, 1755.
(12) Orioli, P. L.; Sacconi, L. *J. Am. Chem. Soc.* **1966**, *88*, 277.
(13) Fox, M. R.; Orioli, P. L.; Lingafelter, E. C.; Sacconi, L. *Acta Crystallogr.* **1964**, *17*, 1159.
(14) Orioli, P. L.; Di Vaira, M.; Sacconi, L. *Inorg. Chem.* **1966**, *5*, 400.
(15) Peisach, J.; Blumberg, W. E. *Arch. Biochem. Biophys.* **1974**, *105*, 691.
(16) (a) Yokoi, H. *Bull. Chem. Soc. Jpn.* **1974**, *47*, 3037. (b) Yokoi, H.; Addison, A. W. *Inorg. Chem.* **1977**, *16*, 1341. (c) Sakaguchi, U.; Addison, A. W. *J. Am. Chem. Soc.* **1977**, *99*, 5189.

0020-1669/92/1331-3138$03.00/0

Table I. EPR and ENDOR Parameters of Copper(II) Complexes and Their Structures

no.	complex	donor set	matrix	structure[a]	ω/ deg[b]	$g_\parallel$	$g_\perp$ or g_x, g_y	$\lvert^{Cu}A_\parallel\rvert$/ MHz	$\lvert^{Cu}A_\perp\rvert$/MHz or $\lvert^{Cu}A_x\rvert$,$\lvert^{Cu}A_y\rvert$	β/ deg[d]
1	$Cu(ipsal)_2$	*trans*-N_2O_2	toluene	THD	120.3[c]	2.232	2.040, 2.076	524	20, 40	25
2	$Cu(ipsal)_2$	(*trans*)N_2O_2	$Ni(ipsal)_2$	THD	98.5	2.281	2.040, 2.098	368	<50, <50	37
3	$Cu(ipsal)_2$	(*trans*)N_2O_2	$Zn(ipsal)_2$	THD		2.281	2.040, 2.098	368	<50, <50	
4	Cu(hapt)	*cis*-N_2O_2	Ni(hapt)	THD		2.212	2.037	588	76	<30
5	Cu(saltn)	*cis*-N_2O_2	Zn(saltn)	THD		2.268	2.062	498	55	34
6	$Cu(msal)_2$	N_2O–O_2	$Zn(msal)_2$	TBP		2.234	2.010, 2.127	424	90, 134	~41
7	$Cu(msal)_2$	*trans*-N_2O_2	$Ni(msal)_2$	SP	0	2.215	2.040, 2.055	598	80, 80	0
8	Cu(acen)	*cis*-N_2O_2	Ni(acen)	SP	0	2.178	2.038	630	97	0
9	Cu(sacen)	*cis*-N_2S_2	Ni(sacen)	SP	0	2.108	2.024	553	114	0
10	Cu(sacen)	*cis*-N_2S_2	Zn(sacen)	THD	55.7	2.126	2.025	494	70	38

[a] Key: SP, square planar; THD, tetrahedral distortion; TBP, trigonal bipyramid. These are structures for the matrix complexes. [b] Dihedral angles between the chelate rings in the matrix molecules, which are obtained from X-ray data. See Figure 15 for the definition. [c] Data for the copper(II) complex. [d] Angle between the principle axes of the **g** and ^{14}N-HFC tensors.

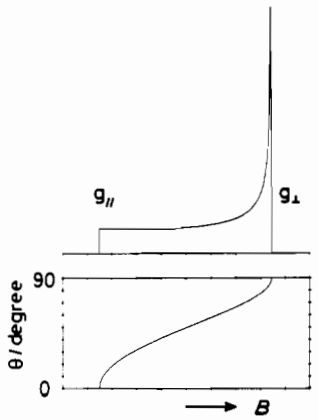

Figure 2. Idealized EPR spectrum with axial symmetric **g** tensor and angle θ dependence of the resonance magnetic field.

Electronic FEM2000 NMR field meter and a Takedariken TR5204 frequency counter, respectively. ENDOR spectra were recorded on an EPR spectrometer equipped with a Varian E1700 ENDOR unit and ENI 550L rf power amplifier by use of rf amplitude modulation. Magnetic field modulation was not used.

In ENDOR measurements for solution samples, the deuterated solvents were used to reduce matrix proton signals. Measurement conditions such as higher copper complex concentration (e.g. 5% rather than 1%), lower temperatures, and high microwave power were effective for enhancement of relative intensities of ^{14}N signals to those of ^{1}H signals, and they were useful to distinguish ^{14}N signals from overlapping ^{1}H signals. Magnetic field dependence of ENDOR signals was also useful to distinguish between ^{14}N and ^{1}H signals, because both signals show quite different magnetic field dependence with respect to each other. The signals assigned to ^{1}H ENDOR are indicated by shading in the ENDOR spectra shown in the figures.

Angle-Selected ENDOR in a Disordered System. Theory. EPR spectra of transition metal complexes in a disordered system usually show anisotropic features. Most copper(II) complexes have large anisotropic **g** and copper HFC tensors, which are nearly axially symmetric. By selecting the magnetic field fixing position on such an anisotropic EPR spectrum, one can observe ENDOR spectra which come from the molecules having a specific orientation with the external magnetic field.[1-4] Figure 2 shows the angle θ dependence of the resonant magnetic field in an idealized EPR spectrum with an axial symmetric **g** tensor. Here, θ is the angle between the external magnetic field and the $g_\parallel$ axis of the molecule. It is easily understood by Figure 2 that the angle θ dependent ENDOR spectra can be observed by changing the magnetic field set position along the resonant magnetic field.

Spectral line shapes of ENDOR in a disordered system were discussed by Hoffman et al.[3] and Kreilick et al.[1] In their papers they dealt with the simplest system of $S = {}^1/_2$ and $I = {}^1/_2$ by deriving the analytical solutions. Recently Hoffman et al. have extended their method to the system containing ^{14}N ($I = 1$).[17] In their analysis of spectra, resonant EPR fields and ENDOR frequencies were treated by a first-order approximation. In the present paper, we use the same method in principle as Hoffman's for analyses of ^{14}N ENDOR spectra, but we treated resonant EPR fields and ENDOR frequencies by the second-order perturbation method, because copper and nitrogen have large HFC constants in the present case.

The spin Hamiltonian for the system is written as

$$\mathcal{H} = \mu_B \tilde{S} g H + h \tilde{S}^{Cu} A^{Cu} I + \sum \{ h \tilde{S}^{N} A^{N} I - \mu_n g_n {}^{N}\tilde{I} H + {}^{N}\tilde{I} {}^{N}Q^{N} I \} \quad (1)$$

where μ_B is the Bohr magneton, h is Planck's constant, μ_N is the nuclear magneton, and g_N is the g factor of the nitrogen nucleus.

The spectral line shapes are represented by the following double integrals:

$$F(H,\nu) = \sum_{m_I(Cu)} \{ \int dg' [S(\theta,\phi) R(H - H_{res}(\theta,\phi)) I(g',\nu)] \} \quad (2)$$

$$I(g',\nu) = \int d\phi \, [U(g',\phi) T(\nu - \nu_{res}(\theta,\phi)) E(\theta,\phi)] \quad (3)$$

In eqs 2 and 3, R and T are the Gaussian or Lorentzian line shape functions for EPR and NMR transitions, respectively, E is the ENDOR enhancement factor defined as square of HFC,[18] and S and U are the anisotropic line shape functions for EPR and NMR transitions expressed by the equations[3a,19]

$$S(\theta,\phi) = \mathrm{Tr}(\tilde{g}g) - (\tilde{h}\tilde{g}g\tilde{g}gh)/g^2 \quad (4)$$

$$U(g,\phi) = \frac{\sin\theta}{(g^2 - g_3^2)\cos\theta} [(g_1^2 - g_2^2)^2 \sin^4\theta \cos^2\phi \sin^2\phi + (g^2 - g_3^2)^2 \cos^2\theta]^{1/2} \quad (5)$$

where the following **g** tensor and the unit vector h in the magnetic field direction are used:

$$\mathbf{g} = \begin{bmatrix} g_1 & & \\ & g_2 & \\ & & g_3 \end{bmatrix} \quad \tilde{h} = [\sin\theta\cos\phi \quad \sin\theta\sin\phi \quad \cos\theta] \quad (6)$$

$$g^2 = \tilde{h}\tilde{g}gh = (g_1^2 \cos^2\phi + g_2^2 \sin^2\phi)\sin^2\theta + g_3^2 \cos^2\theta \quad (7)$$

As mentioned above, we treated H_{res} and rf_{res} by the second-order perturbation method.[19,20]

Model Calculations. The spectral line shape functions, (2) and (3), which are obtained as a function of g and ϕ, are convenient for direct comparison of the calculated spectra with the observed ones, because the experimentally fixed magnetic field does not directly correspond to the angle θ but to the g value. Figure 3a,b shows the results of model calculations of the angle-selected ^{14}N ENDOR spectra for copper(II) complexes containing a nitrogen as one of the donor atoms. The spectra are expressed by $I(g')$ of eq 3, and any convolution about the EPR line shape was not executed. The spin Hamiltonian parameters used for the

(17) Gurbiel, R. J.; Batie, C. J.; Sivaraja, M.; True, A. E.; Fee, J. A.; Hoffman, B. M.; Ballou, D. P. *Biochemistry* **1989**, *28*, 4861.

(18) Whiffen, D. H. *Mol. Phys.* **1966**, *10*, 595.

(19) (a) Rockenbauer, A.; Simon, P. *Mol. Phys.* **1974**, *28*, 1113. (b) Iwasaki, M. *J. Magn. Reson.* **1974**, *16*, 417.

(20) Kita, S.; Hashimoto, M.; Iwaizumi, M. *Inorg. Chem.* **1979**, *18*, 3432.

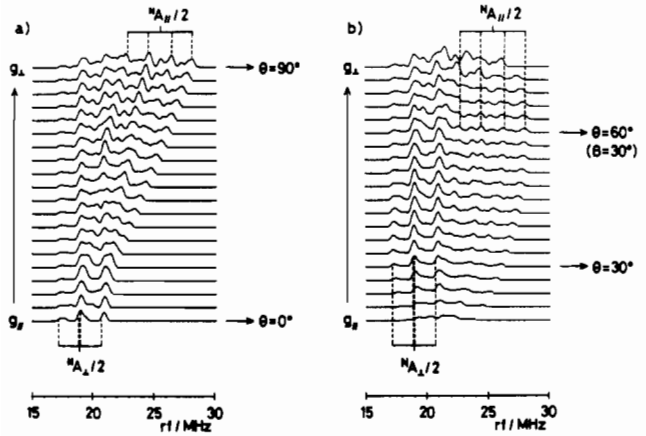

Figure 3. Model calculations of the angle-selected ^{14}N-ENDOR spectra. $I(g,\nu)$ in eq 3 are plotted. In (a) $\beta = 0°$, and in (b) $\beta = 30°$. Other parameters are the same for (a) and (b), and the following values are taken: $g_\parallel = 2.192$; $g_\perp = 2.042$; $|^{Cu}A_\parallel| = -602.9$ MHz; $|^{Cu}A_\perp| = -89.04$ MHz; $^{N}A_\parallel = 50.9$ MHz; $^{N}A_\perp = 37.9$ MHz; $^{N}Q_\parallel = -1.2$ MHz; $^{N}Q_\perp = 0.6$ MHz; $B_0 = 278.6$ mT; microwave frequency = 9.476 GHz; $\gamma_{1/2} = 200$ kHz.

Table II. Atomic Parameters and Spin–Orbit Coupling Constants

atom	orbital	H_{ii}/eV	ζ_1 (C_1)	ζ_2 (C_2)	λ/cm^{-1}
Cu	4s	−11.4	2.2		
	4p	−6.06	2.2		925
	3d	−14.0	5.95 (0.5933)	2.30 (0.5744)	828
S	3s	−20.0	1.82		
	3p	−13.3	1.82		382
O	2s	−32.3	2.275		
	2p	−14.8	2.275		151
N	2s	−26.0	1.95		
	2p	−13.4	1.95		76
C	2s	−21.4	1.625		
	2p	−11.4	1.625		29
H	1s	−13.6	1.3		

calculation were taken from the data of Cu/Ni(salen),[20] but the direction of the ^{14}N HFC tensor was treated as a variable, as for the following.

In the calculation of Figure 3a, the axis for the largest ^{14}N HFC principle value was taken to be pointing toward the copper ion in the $g_\perp$ plane; i.e., the complex was assumed to have a planar coordination structure. In Figure 3b, on the other hand, the axis of the largest ^{14}N HFC principal value was taken to have an angle of 30° with the $g_\perp$ plane. This is a model calculation for the complex with a tetrahedrally distorted coordination structure. One can see from Figure 3 that there are some signal peaks which move according to eq 4, as indicated by the dotted lines, by the change of the magnetic field value. These signals reach the extremes corresponding to the principal value, as the magnetic field value reaches the EPR spectral position where θ is along the ^{14}N HFC principal axis. In Figure 3 the peak positions for the principal values of the ^{14}N HFC tensor are indicated by the arrows. The model calculations apparently indicate that measurements of a series of the angle-selected ENDOR spectra give not only the ^{14}N HFC values but also their orientations relative to the g-tensor axes.

Extended Hückel Molecular Orbital Calculations. Effects of tetrahedral distortion on the electronic structure of the copper(II) binding site were examined also by extended Hückel molecular orbital (EHMO) calculations, for comparison with the ENDOR data. The atomic parameters used for the calculations are listed in Table II, which were taken from literature.[21]

In the calculations, the unpaired electron densities ρ_i were obtained by eq 8, where $C_{\text{somo},i}$ is a coefficient of the ith atomic orbital (AO) of

$$\rho_i = \sum_j C_{\text{SOMO},i} C_{\text{SOMO},j} S_{i,j} \tag{8}$$

the unpaired electron orbital (SOMO) and S_{ij} is the overlap integral between the ith and jth AO's. On the other hand, the hybridization parameter, n^2, of the coordinating orbital was obtained by the following normalized hybrid orbitals expressed on the basis of the bond angles around the nitrogen:[20]

$$\Psi_1^N = n\Phi_s + \sqrt{1-n^2}\Phi_{p_x} \tag{9}$$

$$\Psi_2^N = l\Phi_s + \sqrt{1-l^2}(\Phi_{p_x}\cos\zeta - \Phi_{p_y}\sin\zeta)$$

$$\Psi_3^N = m\Phi_s + \sqrt{1-m^2}(\Phi_{p_x}\cos\eta - \Phi_{p_y}\sin\eta)$$

$$\Psi_4^N = \Phi_{p_z}$$

Here

$$n^2 = \frac{\cos\eta\cos\zeta}{\cos\eta\cos\zeta - \cos\xi} \tag{10}$$

$$l^2 = \frac{\cos\zeta\cos\xi}{\cos\zeta\cos\xi - \cos\eta}$$

$$m^2 = \frac{\cos\xi\cos\eta}{\cos\xi\cos\eta - \cos\zeta}$$

In these expressions, the angles ξ, η, and ζ are defined as in ref 20. The hybridization parameter, n^2, was also determined from the unpaired electron densities on the 2s and 2p orbitals, ρ_{2s} and ρ_{2p}, in the coordinating orbital as

$$n^2 = \frac{\rho_{2s}}{\rho_{2s} + \rho_{2p}} \tag{11}$$

and they can be experimentally determined by the isotropic and anisotropic ^{14}N HFC constants.[22]

On the other hand, the g-tensor components were calculated by eq 12

$$g_{i,j} = g_e\delta_{i,j} + 2\sum_a^{\text{atom}}\sum_k^{\text{orbital}}{}' \frac{\lambda_a\langle\phi_a^{\text{SOMO}}|\hat{l}_a^i|\phi_a^k\rangle\langle\phi_a^k|\hat{l}_a^j|\phi_a^{\text{SOMO}}\rangle}{E_{\text{SOMO}} - E_k} \tag{12}$$

from the extended Hückel MO functions, where g_e is a g value of a free spin, ϕ_a^k is the ath AO in the kth MO, E_k is the orbital energy of the kth MO, and λ_a's are the spin–orbit coupling constants given in Table II. In eq 12, only the one center matrix element of each atom is included. The principal values and the principal axes were obtained by diagonalizing the g tensor.

Experimental Results and Interpretation

EPR Spectra. Yokoi and Addison[16b] and Sakurai and Addison[16c] showed that the $g_\parallel$ values of copper(II) complexes increase and $|^{Cu}A_\parallel|$ values decrease with distortion of the coordination structure from planar to tetrahedral. According to them, the coordination structures of the complexes treated here are regarded as being more distorted from the planar structure in the order **8 < 4 < 5** for the *cis*-N_2O_2 series, **7 < 1 < 2, 3** for the *trans*-N_2O_2 series, and **9 < 10** for the N_2S_2 series. It is apparent that the distortion was realized by doping the copper(II) complexes into the host complexes having tetrahedral distortion even when the guest complexes were square planar when neat. It may be notable that Cu/Zn(msal)$_2$ shows a spectrum typical of a basically $3d_{x^2-y^2}$ ground state, despite that its host complex, Zn(msal)$_2$, has a trigonal bipyramidal coordination structure.[14]

Angle-Selected ENDOR Spectra. (a) *cis*-N_2S_2 Complexes: Cu/Ni(sacen) and Cu/Zn(sacen). In the series of angle-selected ENDOR data for the Cu/Ni(sacen) system (Figure 4a), the signal peak positions at the low rf frequency side did not change with the magnetic field value, while the signal peaks at the highest frequency side move to higher frequencies when the magnetic field set position shifts to the higher field side and they reach an extreme when the spectrum is recorded at the $g_\perp$ extreme. Such

(21) (a) Summerville, R. H.; Hoffmann, R. *J. Am. Chem. Soc.* **1976**, *98*, 7240. (b) Chu, S.-Y.; Hoffmann, R. *J. Phys. Chem.* **1982**, *86*, 1289.

(22) Morton, J. R.; Preston, K. F. *J. Magn. Reson.* **1978**, *30*, 577.

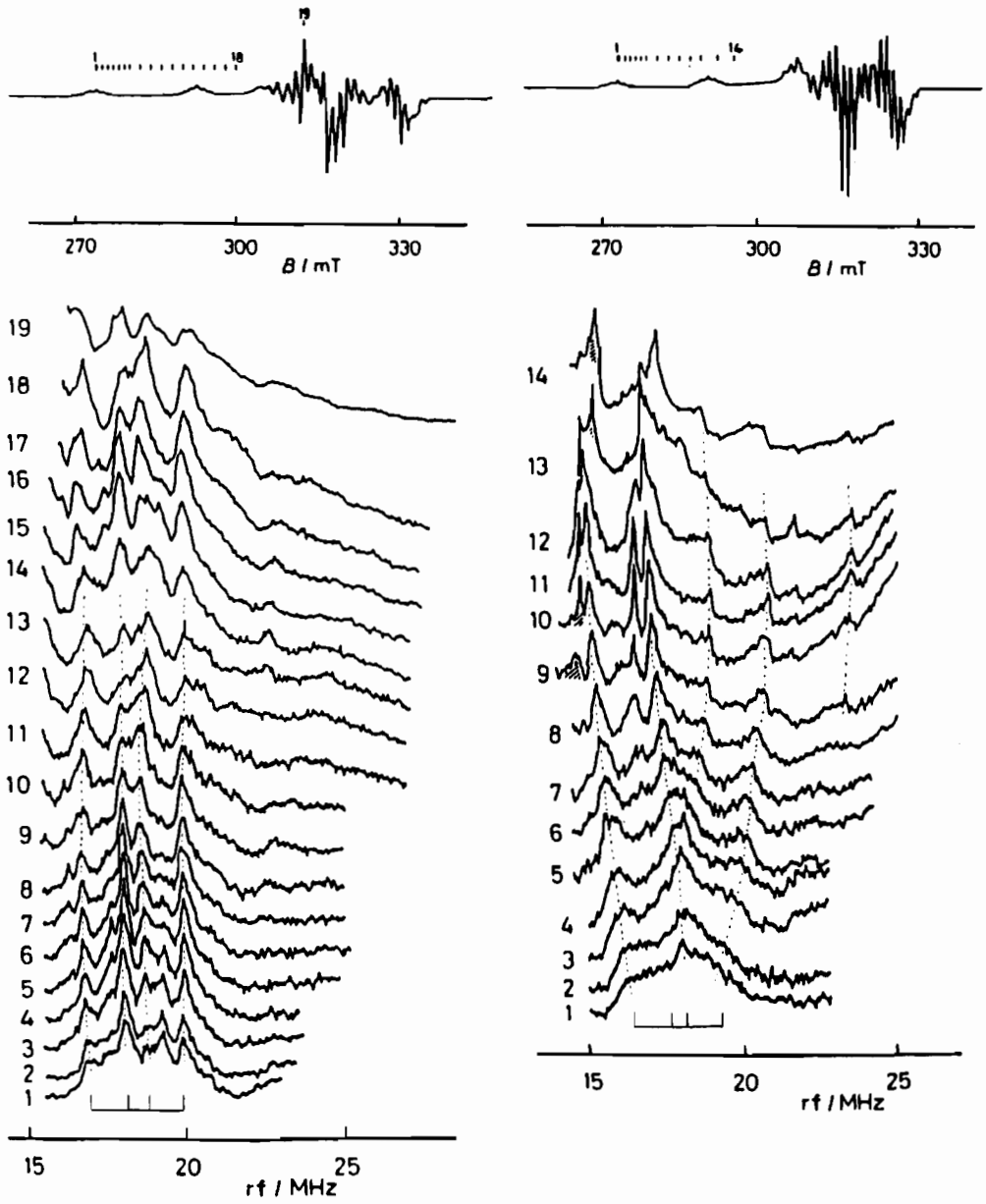

Figure 4. EPR and ENDOR spectra of *cis*-N_2S_2 coordination copper(II) complexes. ENDOR spectra were obtained at the magnetic fields marked on the EPR spectra. Shaded peaks are ^1H signals. (a) Cu/Ni(sacen) measurement conditions: EPR, microwve frequency 8.914 GHz, microwave power 2 mW, field modulation 100 kHz, 5 G_{p-p}, temperature 23.1 K; ENDOR, microwave frequency 8.914 GHz, microwave power 1–2 mW, 1 kHz AM for rf, temperature 19–21 K. (b) Cu/Zn(sacen) measurement conditions: EPR, microwave frequency 8.914 GHz, microwave power 0.2 mW, field modulation 100 kHz, 5 G_{p-p}, temperature 30–28 K; ENDOR, microwave frequency 8.911G Hz, microwave power 0.5 mW, 1 kHz AM for rf, temperature 18.1–18.9 K.

spectral features are similar to those of the model calculations in Figure 3a and indicate that the guest copper(II) complex has a square planar coordination structure. The ^{14}N HFC tensor of the coordinating nitrogen is nearly axial symmetric and coaxial with the g tensor; the principal axis of the smallest ^{14}N HFC is parallel to the $g_\parallel$ axis, while that of the largest one is perpendicular to the $g_\parallel$ axis, respectively.

On the other hand, the features of the angle-selected ^{14}N ENDOR spectra of Cu/Zn(sacen) (Figure 4b) resemble those of the model calculations in Figure 3b. The signal peaks at the low rf frequency side shift toward the lower frequency side by changing the magnetic field set position from $\theta = 0°$ to the larger θ side, and they reach the lowest frequency extreme in the spectrum corresponding to $\theta = 38°$. Here θ's were determined from the θ dependence of the EPR resonant field calculated by the EPR parameters of the complex, which were obtained by spectral simulation of the EPR spectrum. On the other hand, the signal peaks at the high frequency side reach the highest frequency extreme in the spectrum corresponding to $\theta = 50°$. This result indicates that the principal axis for the largest ^{14}N HFC constant has an angle of 50° with the $g_\parallel$ axis, while that of the smallest one has an angle of 40° with the $g_\parallel$ axis, respectively; the angle β between the ^{14}N HFC tensor and the g tensor is estimated to be ~38°.

The difference in the spectral behavior between Cu/Ni(sacen) and Cu/Zn(sacen) reflects the difference between the structures of the host complex molecules. If we assume that the coordination structure of the guest copper(II) complex is the same as that of the matrix molecule and that the principal axis for the largest ^{14}N HFC value is pointing toward the copper ion, the following interesting feature is derived for Cu/Zn(sacen); i.e., the $g_\perp$ plane in Cu/Zn(sacen) nearly coincides with the S–Cu–S plane rather than the mean plane constructed by the four donor atoms as in Figure 14b, which will be shown later as a summary of the $g_\perp$ plane orientations in the different copper binding sites.

(b) *cis*-N_2O_2 Complexes: Cu/Ni(acen), Cu/Ni(hapt), and Cu/Zn(saltn). The angle-selected ^{14}N ENDOR spectra for Cu/Ni(acen) reveal features similar to those in Figure 3a (Figure 5).

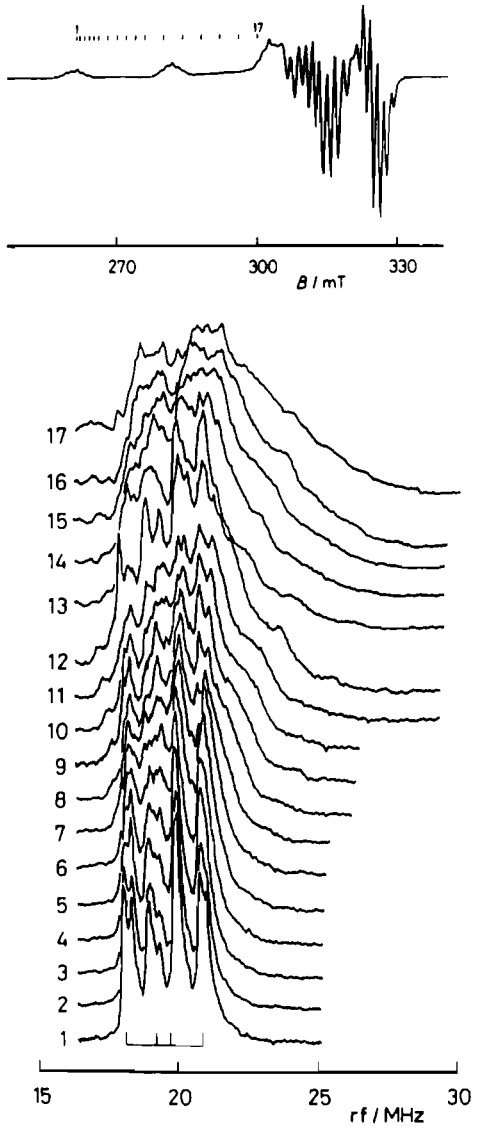

Figure 5. EPR and ENDOR spectra of the *cis*-N_2O_2 coordination Cu/Ni(acen) complex. Measurement conditions: EPR, microwave frequency 8.916 GHz, microwave power 1 mW, field modulation 100 kHz, 5 G_{p-p}, temperature 26.8 K; ENDOR, microwave frequency 8.917 GHz, microwave power, 0.5 mW, 1 kHz AM for rf, temperature 19.9–21.1 K.

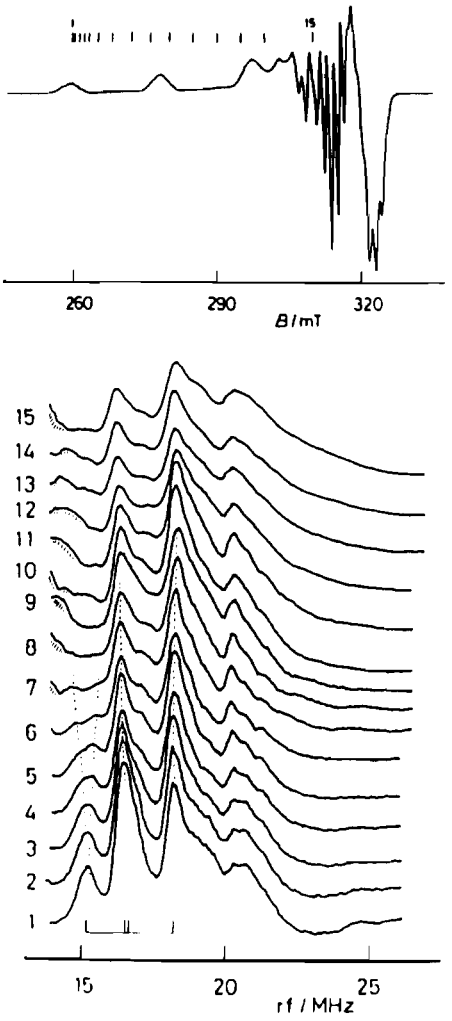

Figure 6. EPR and ENDOR spectra of the *cis*-N_2O_2 coordination Cu/Ni(hapt) complex. Measurement conditions: EPR, microwave frequency 8.910 GHz, microwave power 0.5 mW, field modulation 100 kHz, 5 G_{p-p}, temperature 20.2 K; ENDOR, microwave frequency 8.911 GHz, microwave power 5 mW, 10 kHz AM for rf; temperature 20.0–21.0 K.

This indicates that the complex has the square planar coordination structure as in the host complex,[8] and the tensor axes of the minimum and the maximum ^{14}N HFC values are along the $g_\parallel$ axis and on the $g_\perp$ plane, respectively, as is shown in Figure 14a (vide infra).

The spectral features of the angle-selected ENDOR of Cu/Ni(hapt) are also like those of square planar type complexes (Figure 6), but the behavior of the lowest frequency peak is somewhat different; as the field set position shifts from $g_\parallel$ extreme ($\theta = 0°$) toward the $g_\perp$ region, the main signal peak at ~15 MHz splits into two broad peaks. One moves toward the low-frequency side and the other moves to the high-frequency side. This indicates that the coordination structure is nearly square planar but small distortions may exist or there may be displacement from the axial symmetry in the nitrogen HFC tensor. The value of β is estimated to be less than 30° from the ENDOR spectra.

On the other hand, the angle-selected ENDOR spectra of Cu/Zn(saltn) (Figure 7) are rather similar to those of the model calculation of Figure 3b, indicating the presence of tetrahedral distortion at the copper binding site, as was estimated from the EPR spectra. The value of β is found to be 34° from the angle-selected ENDOR data. By the use of this β value and by taking the same assumptions as those taken for Cu/Zn(sacen), one can conclude that the $g_\perp$ plane is on the mean plane constructed by the four donor atoms (Figure 14c; vide infra).

(c) *trans*-N_2O_2 Complexes: Cu/Ni(msal)$_2$, Cu(ipsal)$_2$/Toluene, Cu/Ni(ipsal)$_2$, and Cu/Zn(ipsal)$_2$. The angle-selected ^{14}N ENDOR spectra of Cu/Ni(msal)$_2$ have characteristic features similar to those of the Figure 3a, indicating that the complex has a square planar coordination structure (Figure 8).

For Cu(ipsal)$_2$, the angle-selected ^{14}N ENDOR spectra recorded from the frozen toluene solution (Figure 9) showed rather broad signals compared to those of most complexes doped in crystals, indicating the presence of disorder in the complex structure in the frozen solution. The behavior of the signals at the low-frequency edge by the change of the magnetic field set position indicates that the ^{14}N HFC tensor is noncoaxial with the g tensor, and hence the coordination structure in solution may be distorted from square planar as in the neat crystal, where the dihedral angle ω between the two N–Cu–O planes is known to be 120.3°.[12] The angle β in the solution state was estimated from the ENDOR spectra to be 25°. One can estimate from this β value by the same manner as used above that the $g_\perp$ plane is on the mean plane constructed by the four donor atoms.

On the other hand, the Cu(ipsal)$_2$ complex doped in nickel and the zinc complexes (Cu/Ni(ipsal)$_2$ and Cu/Zn(ipsal)$_2$) showed EPR spectra with marked rhombic features, and hence the ENDOR spectra were recorded by changing the magnetic field set position from both sides, the low-field side and the high-field side (Figures 10 and 11).

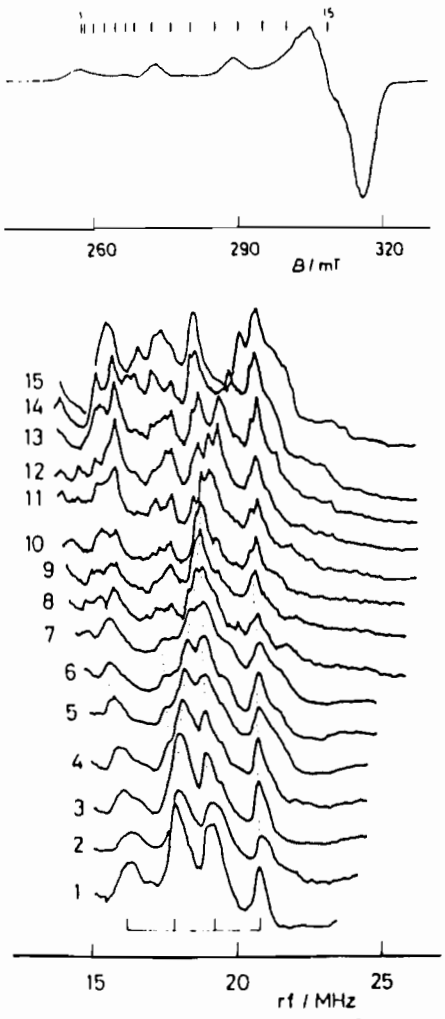

Figure 7. EPR and ENDOR spectra of the *cis*-N_2O_2 coordination Cu/Zn(saltn) complex. Measurement conditions: EPR, microwave frequency 8.921 GHz, microwave power 0.5 mW, field modulation 100 kHz, 5 G_{p-p}, temperature 21.3 K; ENDOR, microwave frequency 8.921 GHz, microwave power 20 mW, 10 kHz AM for rf, temperature 20.3–21.6 K.

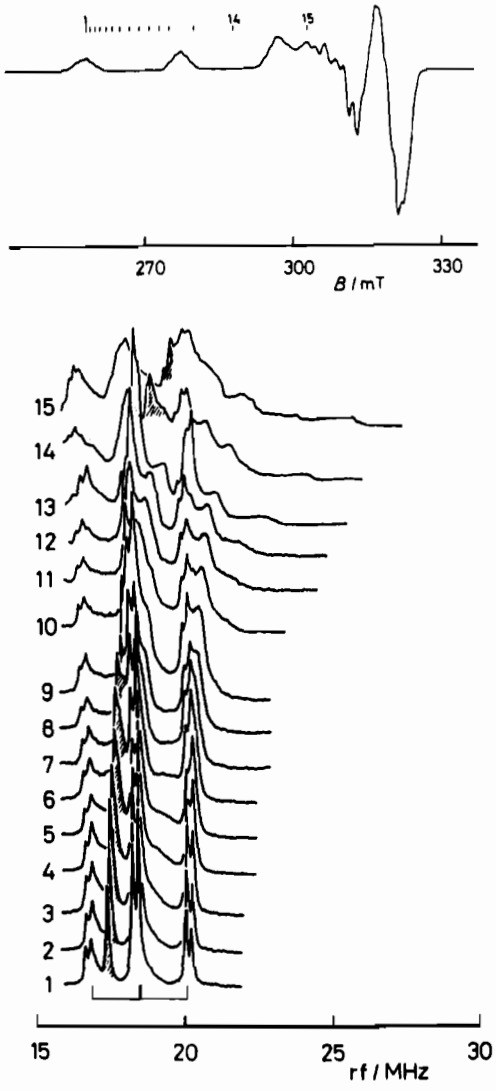

Figure 8. EPR and ENDOR spectra of the *trans*-N_2O_2 coordination Cu/Ni(msal)$_2$ complex. Measurement conditions: EPR, microwave frequency 8.915 GHz, microwave power 0.2 mW, field modulation 100 kHz, 5 G_{p-p}, temperature 18 K; ENDOR, microwave frequency 8.915 GHz, microwave power 0.2 mW, 1 kHz AM for rf, temperature 19.2–20.2 K.

As Figures 10 and 11 show, the magnetic field dependence of the ENDOR spectra is very different from those of the square planar and slightly distorted complexes; all the ENDOR signals are concentrated in the small rf frequency range at the low-frequency region. Such features indicate that the ^{14}N HFC constant and its anisotropy are much smaller than those for ordinary square planar or slightly distorted complexes, and they are more remarkable in the nickel and zinc complex matrices than in the toluene solution. Meanwhile, the nickel and zinc host complexes may have similar copper binding sites because their EPR spectral features and the angle θ dependence of ^{14}N ENDOR signals are similar to each other.

The Ni(ipsal)$_2$ complex is known to have a dihedral angle of 98.5°,[13] which is the angle between the two chelate rings. Such a large distortion from tetrahedral is well revealed by the β value, which was estimated to be 37° from the ENDOR data. The large β value and the surprisingly small HFC constant (Table III) indicate that the donor nitrogens in these systems are largely out of the plane of the copper unpaired electron orbital, and the overlap between the copper and the nitrogen orbitals is small. The small anisotropic features indicate also that there is little spin density on the nitrogen 2p orbitals. From the β value, the $g_\perp$ plane was estimated to be on the mean plane constructed by the four donor atoms by the same assumptions taken for Cu/Zn(sacen) (Figure 14d).

(d) Trigonal Bipyramidal O–N_2O–O Complex: Cu/Zn(msal)$_2$. The host Zn(msal)$_2$ complex has a trigonal bipyramidal coordination structure,[14] and hence the guest copper(II) complex, which originally has a square planar structure, was expected to have a largely distorted coordination structure. It is known that some trigonal bipyramidal copper complexes have the d_{z^2} ground state. However, Cu/Zn(msal)$_2$ showed an EPR spectrum characteristic of the $d_{x^2-y^2}$ ground state of $g_\parallel(g_z) > g_\perp(g_x,g_y)$ and $A_\parallel(A_z) > A_\perp(A_x,A_y)$, but it has a large rhombic distortion. It seemed interesting to examine such a system by the angle-selected ENDOR method.

The angle-selected ENDOR spectra were recorded from both sides of the EPR spectrum, from the low-field side and the high-field side. The recorded ENDOR spectra are shown in Figure 12. The ^{14}N HFC constants were determined to be a_{iso} = 25 MHz and b_{aniso} = 1.3 MHz, respectively. These HFC constants and anisotropy are as small as those in Cu/Ni(ipsal)$_2$ and Cu/Zn(ipsal)$_2$, meaning that the overlap between the copper and the nitrogen orbitals is small; the orbital lobe of the copper $3d_{x^2-y^2}$ orbital would not be extending toward the donor nitrogen atoms.

EHMO calculations were executed for $[Cu(NH_3)_2(H_2O)_3]^{2+}$ [21] by taking it as a model complex of trigonal bipyramidal complex with the O–N_2O–O donor set. In the calculations, all the Cu–N and Cu–O bond lengths were taken to be 2.0 Å and the trigonal plane was constructed by $(NH_3)_2(H_2O)$. The calculational result shows that the copper unpaired electron orbital mainly consists

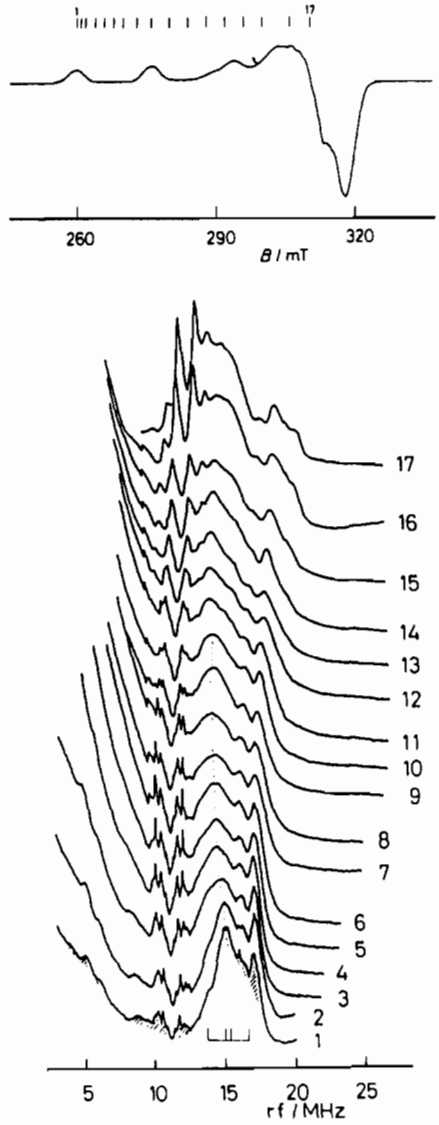

Figure 9. EPR and ENDOR spectra of the *trans*-N_2O_2 coordination $Cu(ipsal)_2$ complex in frozen toluene-d_8 solution. Measurement conditions: EPR, microwave frequency 8.909 GHz, microwave power 5 mW, field modulation 100 kHz, 5 G_{p-p}, temperature 28.4 K; ENDOR, microwave frequency 8.909 GHz, microwave power 10 mW, 1 kHz AM for rf, temperature 21.3–23.3 K.

of the $3d_{z^2}$ orbital (Figure 13a), but if the donor nitrogens in the equatorial plane move so as to increase the N–Cu–N angle, the copper unpaired electron orbital changes to predominantly $3d_{x^2-y^2}$ (Figure 13b).[23] The latter is the case observed for Cu/Zn-$(msal)_2$, and hence the copper binding site in the zinc(II) complex may have a somewhat different coordination structure compared to the host zinc(II) complex, as is shown in Figure 14e (vide infra).

It is known that the copper binding sites in *P. nigra* plastocyanin and *A. denitrificans* azurin have a N_2S–S trigonal pyramidal and a O–N_2S–S trigonal bipyramidal structure, respectively. In these cases the trigonal planes have a N_2S donor set and the axial ligands are situated further from the copper ions than those in the present case. The EHMO calculations for the copper binding sites in these blue copper proteins give features different from the present one; the unpaired electron orbital is on the equatorial trigonal plane, but it is largely deformed by the effects of the ligand fields, especially by the effect of sulfurs.[24b] In the present case, the unpaired electron is not on the trigonal N_2O_{eq} plane but on the plane perpendicular to it. This may be due to the fact that the tetragonal pyramidal $N_2(O_{ax})_2$–O_{eq} crystal field would be stronger than the O_{ax}–N_2O_{eq}–O_{ax} trigonal bipyramidal crystal field because of the large N–Cu–N angle close to 120°. This result indicates that the copper electronic states can be largely affected by the donor atoms as well as their configuration.

(23) $d_{x^2-y^2}$ and d_{z^2} orbitals are not hybridized ones but are obtained by unitary transformation of $d_{x^2-y^2}$ and d_{z^2}.

Discussion

Effects of Tetrahedral Distortion on ^{14}N HFC Constants and Unpaired Electron Distribution. Table III shows that tetrahedral distortion decreases the ^{14}N HFC constants and hence the unpaired electron densities on the coordinating nitrogens. Their decreases are especially remarkable in the $Cu/Ni(ipsal)_2$, $Cu/Zn(ipsal)_2$ and $Cu/Zn(msal)_2$ complexes.

For comparison with the experimental data, the EHMO calculations were executed. The calculations were made for the model complexes, and tetrahedral distortion was realized by twisting the chelating ligands (Figure 15). The unpaired electron densities obtained as a function of tetrahedral distortion are shown in Figure 16a. The results apparently indicate that the unpaired electron density on the nitrogen 2s orbital decreases by tetrahedral distortion, and as the distortion becomes larger, the densities decrease more markedly. This is consistent with the experimental results which show that the ^{14}N HFC constant decreases more markedly as the distortion becomes larger as in the cases of $Cu(ipsal)_2$ and $Cu(msal)_2$. Though the calculated unpaired electron densities are not coincident quantitatively with the experimental ones, the ratios between the unpaired electron densities for the distorted structures and those for the planar structure are in good agreement with the experimental ones. It should be noticed that the effects of tetrahedral distortion on spin distribution remarkably differ between the N_2S_2 donor set system and the N_2O_2 system.

In the previous paper,[24] we showed that there is a good correlation between the types of donor sets and ^{14}N HFC parameters of the donor nitrogens obtained from single crystal like ENDOR spectra, which are recorded by setting the magnetic field at the $g_\parallel$ extreme. The correlation was useful to estimate or confirm the donor sets in copper(II) complexes with unknown or uncertain coordination structures. We pointed out, however, that the correlation may not be necessarily effective to find tetrahedral distortion, because the effects of tetrahedral distortion on the ^{14}N HFC parameters obtained from the turning point of the spectra were not so remarkable as far as the distortion is small. This is well understood by the present data as indicated by the following.

In the square planar complexes, the ^{14}N HFC parameters obtained from the $g_\parallel$ extreme correspond to the principal values of the ^{14}N HFC tensors, $^{N}A_\perp$, while, in the tetrahedrally distorted cases ($\beta \neq 0$), the observed HFC parameters obtained by the method contain a contribution of $^{N}A_\parallel$, which is much larger than $^{N}A_\perp$, according to eq 13. Hence, despite that the principal values

$$[^{N}A(\theta)]^2 = {}^{N}A_\perp{}^2 \cos^2(\theta-\beta) + {}^{N}A_\parallel{}^2 \sin^2(\theta-\beta) \qquad (13)$$

become smaller with tetrahedral distortion, the HFC parameters obtained by the turning point method do not reflect the decrease of the principal values as far as the tetrahedral distortion is small. This can be seen in the ENDOR spectra of Cu/Zn(sacen); the spectrum observed at the $g_\parallel$ extreme showed signals at nearly the same frequency range as those observed for Cu/Ni(sacen), despite that the principal value in the former is appreciably smaller than that in the latter. However, it should be noticed that when the

(24) (a) Iwaizumi, M.; Kudo, T.; Kita, S. *Inorg. Chem.* **1986**, *25*, 1546. (b) Miyamoto, R.; Ohba, Y.; Iwaizumi, M. *Inorg. Chem.* **1990**, *29*, 3234.

(25) In the previous paper,[24b] we reported that $^{N}A_\perp$ = 38.4 MHz for Cu/Ni(sacen), but it should be replaced by 37.0 MHz, which was obtained under better S/N conditions in the present work.

(26) Though the signals were undoubtedly assigned to ^{14}N ENDOR, a reliable analysis of the angle-dependent ENDOR could not be made.

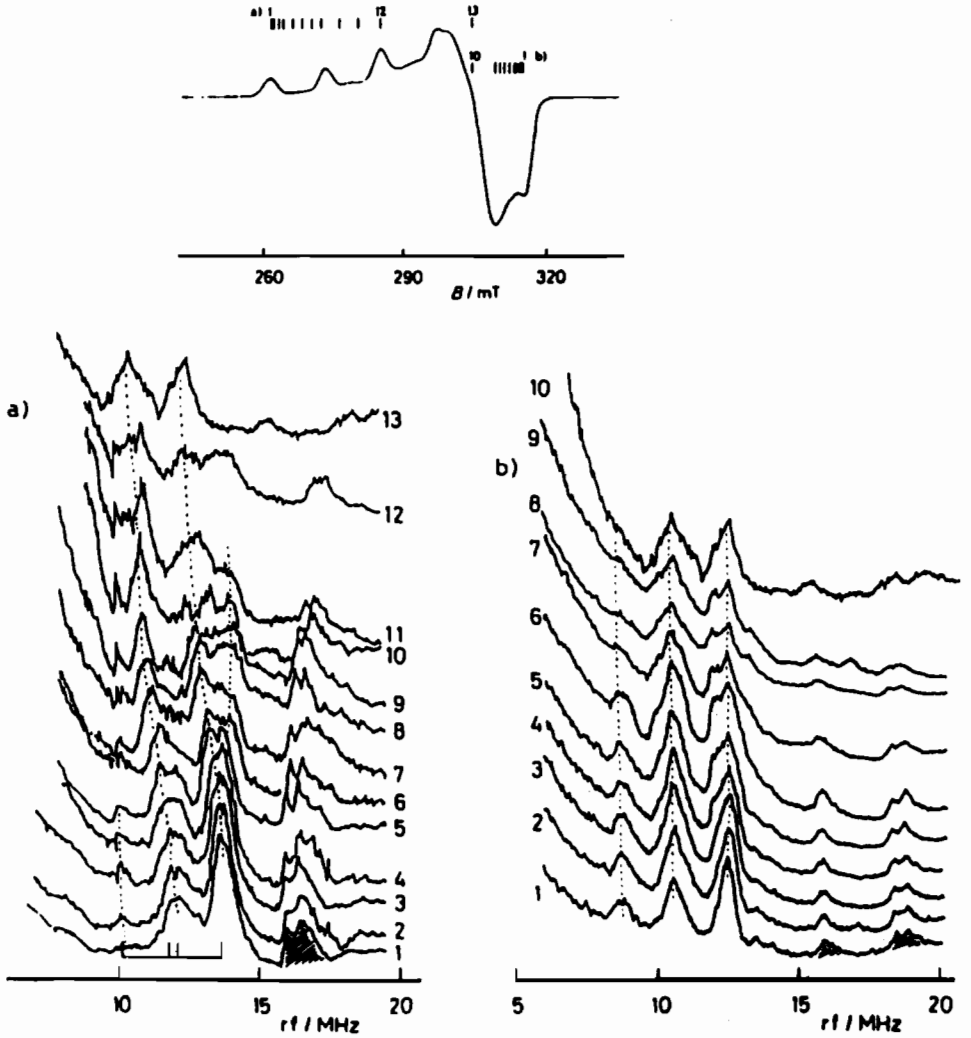

Figure 10. EPR and ENDOR spectra of the *trans*-N_2O_2 coordination Cu/Ni(ipsal)$_2$ complex. Measurement conditions: EPR, microwave frequency 8.909 GHz, microwave power 2 mW, field modulation 100 kHz, 5 G_{p-p}, temperature 14.6 K; ENDOR, microwave frequency 8.910 GHz, microwave power 20 mW, 10 kHz AM for rf, temperature 14.4–16.5 K.

distortion becomes large, the HFC parameters obtained from the $g_{\parallel}$ extreme will become appreciably small as was seen in Cu/Ni(ipsal)$_2$, Cu/Zn(ipsal)$_2$, or Cu/Zn(msal)$_2$.

Hybridization of the Coordinating Nitrogen Orbitals. The hybridized states of the coordinating nitrogen orbitals which were evaluated from both the unpaired electron distribution on the nitrogen 2s and 2p orbitals and bond angles around the nitrogen atoms by eq 10 are listed in Table III. It shows that most of the n^2 values obtained from the ENDOR data are roughly in agreement with those estimated from the X-ray crystallographic data except for the case of Cu/Ni(ipsal)$_2$ and Cu/Ni(msal)$_2$, though the EHMO method gives much smaller n^2 values than those experimentally evaluated, but they show some interesting features.

Figure 16b shows the n^2 values calculated by the EHMO method as a function of tetrahedral distortion, and it indicates that the n^2 value becomes smaller with tetrahedral distortion, through the bonding angles around the coordinating nitrogen are kept constant in the calculations. This suggests that the hybridized orbitals of nitrogen may be expressed in somewhat sp^3-like orbitals rather than in the sp^2-like orbitals of eq 9. It means that the lobe of the coordinating nitrogen orbital may not be necessarily pointing toward the copper nucleus, but toward the position of the maximum density of the copper unpaired electron orbital, so as to form a banana-like bond. It must be noticed that the copper unpaired electron orbital has less tendency to deform tetrahedrally, since mixing of the $4p_z$ orbital with the $d_{x^2-y^2}$ unpaired electron orbital is required for tetrahedral deformation. The hole in the 3d orbitals (the unpaired electron orbital) tends to be placed in the direction of the highest crystal field, while electron distribution among the vacant 4s and 4p orbitals would occur so as to make minimum the crystal field from the donor atoms. Hence, the electronic lobe of the hybridized orbital would point toward the middle of the donor atoms. Therefore, such orbital mixing would not work to diminish the banana-like bonding.

It was mentioned above that the n^2 values obtained from the ENDOR data for Cu/Ni(ipsal)$_2$ and Cu/Ni(msal)$_2$ disagree with those obtained from X-ray crystallographic data. For Cu/Ni(msal)$_2$, which has a planar coordination structure, the reason is not clear, but the disagreement in Cu/Ni(ipsal)$_2$, which has a largely tetrahedrally distorted structure, may imply the formation of the banana-like bond.

The ENDOR spectra observed for the complexes having largely distorted coordination structures seemed to be less anisotropic. This may be mostly due to the fact that the absolute magnitude of the anisotropic component becomes small when accompanied by a decrease of unpaired electron densities on the nitrogens.

Orientation of the g Tensor and the Unpaired Electron Orbitals in the Molecular Framework. The g tensor gives important information on the copper unpaired electron orbital. As it is mainly determined by the spin–orbit interactions of the 3d electrons of the metal, orientation of the g tensor is largely related to orientation of the unpaired electron orbital.

In d^9 complexes, the unpaired electron orbital, i.e., the hole in the 3d orbitals, is situated in the direction of the strongest ligand field. In square planar complexes, therefore, the $g_{\perp}$ plane is on

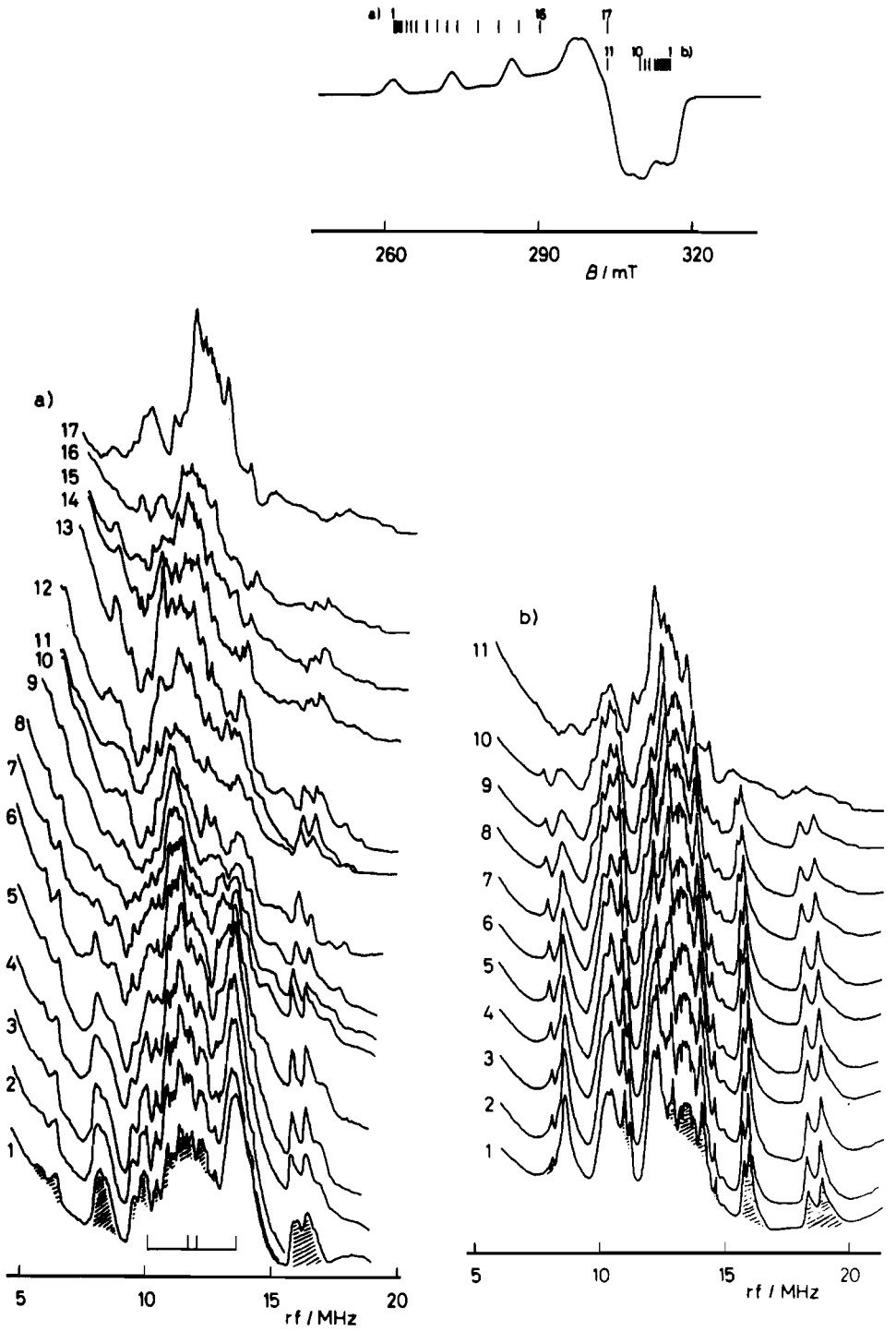

Figure 11. EPR and ENDOR spectra of the *trans*-N_2O_2 coordination Cu/Zn(ipsal)$_2$ complex. Measurement conditions: EPR, microwave frequency 8.908 GHz, microwave power 5 mW, field modulation 100 kHz, 5 G_{p-p}, temperature 20.4 K; ENDOR, microwave frequency 8.908 GHz, microwave power 5 mW, 1 kHz AM for rf, temperature 19.6–21.3 K.

the square planar molecular plane. However, few investigations have been reported on the orientation of the unpaired electron orbital in complexes having a highly distorted coordination structure. The examination of orientation of the unpaired electron orbital in such a distorted structure system seems interesting, and important problems exist in connection with the electronic states of copper binding sites in copper proteins, because most of copper proteins have copper binding sites of distorted coordination structures and the electronic states in such environments must be correlated to their enzymatic functions. For example, in blue copper proteins, which have functions in electron transport, the orientation of the unpaired electron orbital in the coordination framework may be related to the electron pathway.

It was shown above that, in the tetrahedrally distorted N_2S_2 complex, the $g_\perp$ plane may be on the S–Cu–S plane. However, it is not clear whether the $g_\perp$ plane corresponds directly to the plane of the unpaired electron orbital or not in such distorted copper binding sites. We examined the orientation of the g tensor and the copper unpaired electron orbital by the EHMO calculations for a model complex. Figure 16c shows the orientation of the $g_\parallel$ axis in the framework of the donor atoms obtained by the EHMO calculation, where the y axis was taken to be normal to the molecular plane of the planar *cis*-N_2X_2 (X = O, S) type complexes, as is shown in Figure 15. Tetrahedral distortion of the coordination structure was realized by rotating symmetrically the two coordinating N–Cu–X (X = O, S) planes about the x axis toward opposite directions with respect to each other. The black marks indicate the orientation of the $g_\parallel$ axis

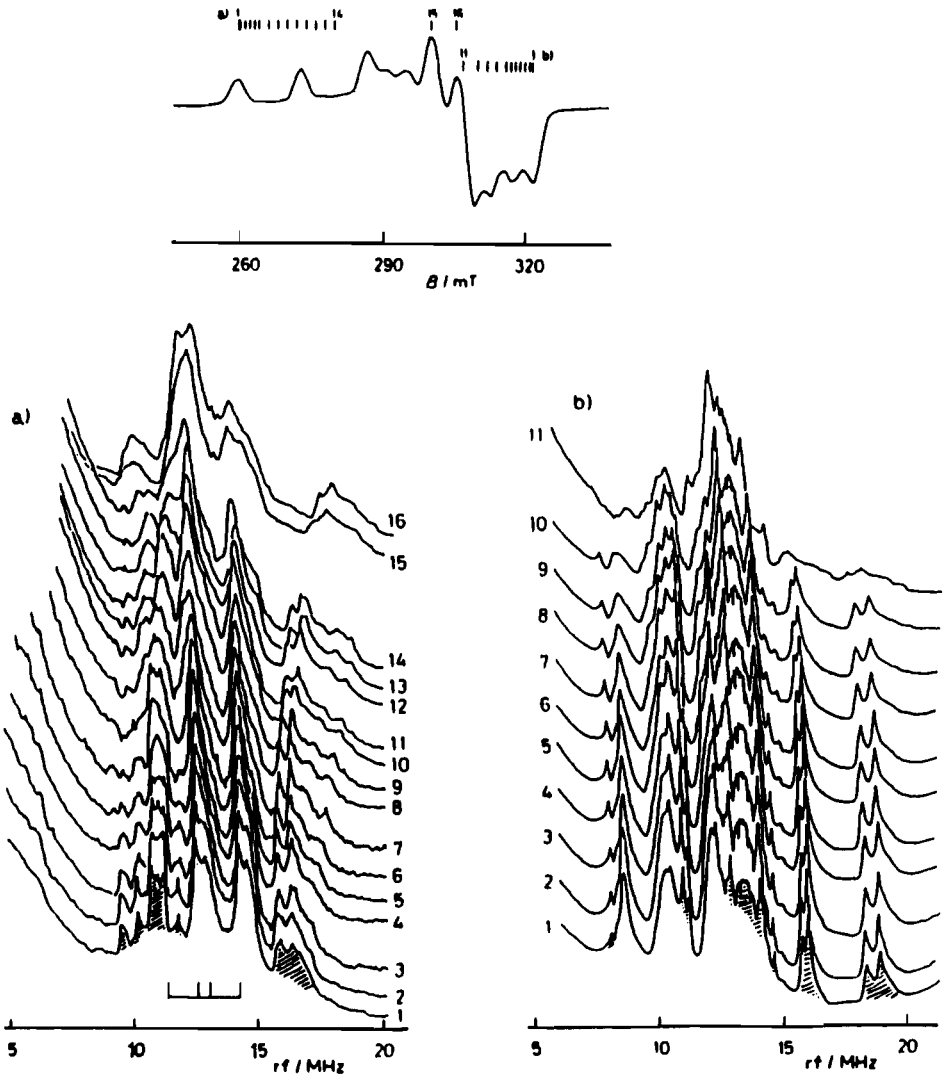

Figure 12. EPR and ENDOR spectra of the trigonal bipyramidal N_2O–O_2 coordination Cu/Zn(msal)$_2$ complex. Measurement conditions: EPR, microwave frequency 8.910 GHz, microwave power 1 mW, field modulation 100 kHz, 5 G_{p-p}, temperature 20.2 K; ENDOR, microwave frequency 8.909 GHz, microwave power 10 mW, 1 kHz AM for rf, temperature 19.7–21.9 K.

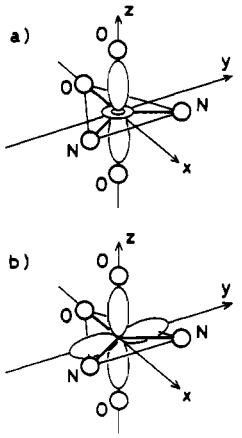

Figure 13. Copper unpaired electron orbital in a trigonal bipyramidal N_2O–O_2 coordination structure. The orbitals are (a) d_{z^2} and (b) $d_{x^2-y^2}$.

calculated by taking into account only the copper orbitals; but the open marks were obtained by taking into account also the spin–orbit coupling effects of the donor atoms. The former corresponds to the orientation of the copper unpaired electron orbital, while the later corresponds to the real orientation of the g tensor.

Figure 16c indicates that the unpaired electron orbital in the N_2S_2 complexes may be on the mean plane constructed by the four donor atoms, but the $g_\perp$ plane tilts toward the S–Cu–S plane. The experimental results suggest that the copper unpaired

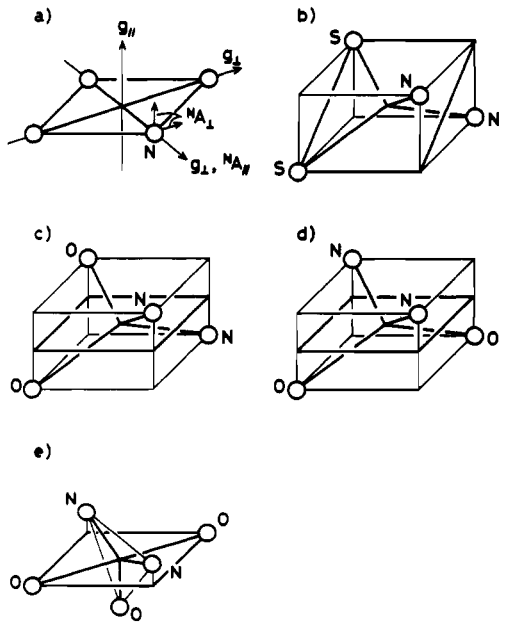

Figure 14. Schematic coordination structure of the copper complexes and $g_\perp$ plane direction. $g_\perp$'s are indicated by the bold-lined tetragonal. Coordination structures are (a) square planar, (b) tetrahedrally distorted *cis*-N_2S_2, (c) tetrahedrally distorted *cis*-N_2O_2, (d) tetrahedrally distorted *trans*-N_2O_2, and (e) trigonal bipyramidal N_2O–O_2.

Table III. ^{14}N Hyperfine Coupling Constants, Spin Densities, and Hybridization Parameters

no.	complex	$^{N}A_{\parallel}$/ MHz	$^{N}A_{\perp}$/ MHz	$^{N}A(g_{\parallel})$/ MHz[a]	β/ deg[b]	a_{iso}/ MHz[c]	b_{aniso}/ MHz[c]	ρ_{2s}/ %[d]	ρ_{2p}/ %[d]	n^2 [e]	$n_{cryst}{}^2$ [f]
1	$Cu(ipsal)_2$/toluene	33.8	29.6	30.4	25	31	1.4	~1.7	~2.5	~0.40	0.45, 0.39
2	$Cu/Ni(ipsal)_2$	27.0	21.8	23.8	37	23.5	1.7	1.30	3.06	0.30	0.40, 0.44
3	$Cu/Zn(ipsal)_2$	~27	~22	~24	~37	~24	~1.7	~1.3	~3.0	~0.30	
4	Cu/Ni(hapt)	*h*	*h*	~33	*h*						
5	Cu/Zn(saltn)	42.9	34.0	37.0	34	37.0	3.0	2.04	5.40	0.27	
6	$Cu/Zn(msal)_2$	~28	~24	~26	~41	~25	~1.3	~1.4	~2.4	~0.37	0.37, 0.36
7	$Cu/Ni(msal)_2$	46.5	37.0	37.0	0	40.2	3.2	2.22	5.76	0.28	0.40
8	Cu/Ni(acen)	48.7	39.1	39.1	0	42.6	3.2	2.35	5.76	0.29	0.32, 0.31
9	Cu/Ni(sacen)	49.0	37.0[g]	37.0	0	41.0	4.0	~2.3	~7.2	~0.24	0.33, 0.33
10	Cu/Zn(sacen)	39.9	33.0	36.0	38	35.3	2.3	1.95	4.14	0.32	0.28

[a] ^{14}N-HFC parameters observed at the $g_{\parallel}$ position of EPR spectra. [b] Angle between the principal axes of the g tensor and the ^{14}N-HFC tensor. [c] Calculated from the equations $a_{iso} = (A_{\parallel} + A_{\perp})/3$ and $b_{aniso} = (A_{\parallel} - A_{\perp})/3$. [d] Calculated from the equations[22] $\rho_{2s} = a_{iso}/1811$ MHz and $\rho_{2p} = b_{aniso}/55.52$ MHz. [e] Calculated from eq 11 in the text. [f] Calculated from eq 10 in the text. Two values are for the crystallographically inequivalent two coordinating nitrogens. [g] See ref 25. [h] See ref 26.

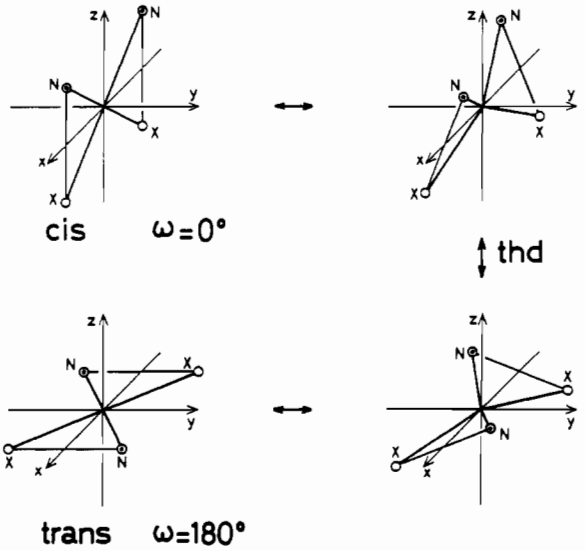

Figure 15. Tetrahedrally distorted N_2X_2 coordination structures of model complexes for EHMO calculations (X = O, S). ω is the dihedral angle between N–Cu–X chelating planes. It is defined as $\omega = 0°$ for *cis*-N_2X_2 planar complexes and $\omega = 180°$ for *trans*-N_2X_2 ones. The *y* axis is normal to the planar *cis*-N_2X_2 complex, while the *z* axis is normal to the planar *trans*-N_2X_2 complex.

electron orbital would be tilting toward the S–Cu–S plane by the ligand field of the sulfurs stronger than the nitrogens. However, the results of the EHMO calculation do not show such an appreciable tilt of the unpaired electron orbital. This may be due to that the EHMO method takes the ligand field of sulfurs to be more minor than the actual case. It should be notable, however, that the EHMO calculation indicates that tilt of the $g_{\perp}$ plane is related to the marked spin–orbit coupling effect of the coordinating sulfurs, because the appreciable spin densities are populating them and the sulfurs have a large spin–orbit coupling constant. This result seems important when considering the electronic states of the copper binding sites in the distorted coordination system containing sulfurs as donor atoms.

On the other hand, as Figure 16c shows, the orientations of the calculated $g_{\perp}$ plane and the unpaired electron orbital are in coincidence with each other in the N_2O_2 type complexes; the coordinating atoms do not make significant contributions to the g tensor. This is due to the fact that spin densities populating the donor atoms are little in addition to that the spin–orbit coupling constants of nitrogen and oxygen atoms are small. It was shown from the experimental results that the $g_{\perp}$ plane in the N_2O system may be in the average plane of the donor atoms. However, the EHMO calculations indicate that the $g_{\perp}$ plane may be displaced from the mean plane of the donor atoms toward the N–Cu–N plane. This is because nitrogen gives a stronger ligand field than oxygen does. The discrepancy between the ENDOR analyses and the MO calculations may be due to that in the EHMO calculations the effects of the nitrogen ligand field were being taken into account excessively or it may arise from the fact that there may be banana-like bonds between copper and nitrogen which may introduce some errors in the analysis of the orientation of the unpaired electron orbital by ENDOR data. However, with the absence of X-ray data for the *cis*-N_2O_2 type complexes treated here, one can not say much about them.

It seems valuable to mention here that Cu/Zn(sacen) and $Cu/Ni(ipsal)_2$ have nearly the same β values but the latter has much a smaller ^{14}N HFC constant (Table III). This may be related

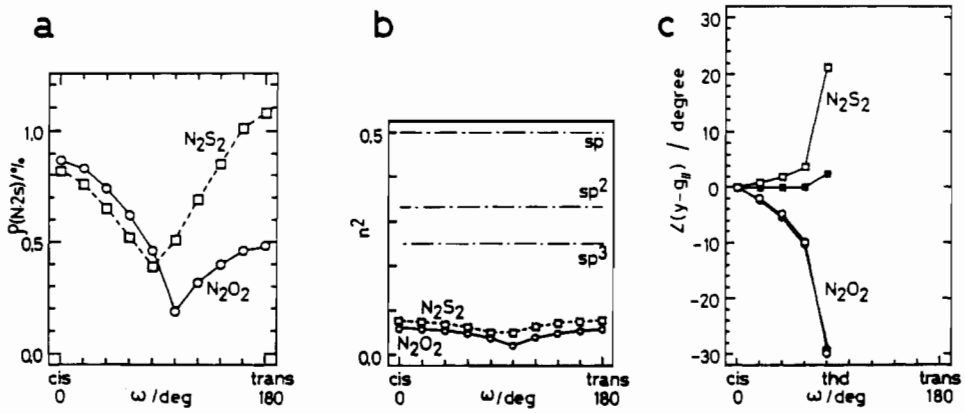

Figure 16. Structural parameters obtained from EHMO calculations for model complexes as a function of tetrahedral distortion: (○) N_2O_2; (□) N_2S_2. In (a) ρ_{2s} is calculated from eq 8. In (b) the n^2 value of coordinating nitrogen is calculated from eqs 8 and 11. n^2 values expected for sp-, sp^2-, and sp^3-hybridization are indicated by the horizontal lines, respectively. In (c) $g_{\parallel}$ directions are obtained by diagonalization of the g tensor calculated from eq 12. Open marks are for results where the spin–orbit couplings of copper and donating atoms were taken into account; closed marks are for results where only the spin–orbit coupling of the copper atom was taken into account.

to the fact mentioned above that in the N_2S_2 donor set system the $g_\perp$ plane is displaced from the plane of the unpaired electron orbital and tilts toward the S–Cu–S plane, but in the N_2O_2 complexes the plane of the unpaired electron orbital and the $g_\perp$ plane coincide with each other. That is, the nitrogen in the Cu/Zn(sacen) system is situated closer to the unpaired electron orbital than the nitrogen in Cu/Ni(ipsal)$_2$, despite that the β values are nearly the same.

Acknowledgment. The present work was partially supported by Grant-in-Aid for Scientific Research No. 02453036 from the Ministry of Education, Science, and Culture of Japan.